May 2026

Cosmological Evolution of Glueball Dark Matter in Dark Yang-Mills Sectors

Calla Geimer

Theoretical Particle Physics
Department of Physics
Lund University

Bachelor's thesis (15 hp) supervised by Roman Pasechnik

Abstract

This thesis investigates the possibility of dark matter arising from a confining dark $SU(N)$ Yang-Mills sector with $N = 3, 4, 5$. First, standard results from the established single-scalar-glueball framework are reviewed and numerically reproduced in order to follow the cosmological evolution through the confinement phase transition and extract the relic abundance. The results reproduce the expected qualitative behaviour for the relic abundance which shows that glueballs could account for the totality of dark matter. The analysis is then extended at an exploratory level to a two-glueball effective theory which contains scalar and pseudoscalar degrees of freedom. For this two-field case, coupled equations of motion are solved for benchmark parameter choices. Since the two-field temperature potential is not yet lattice calibrated, and since the late-time oscillatory regime is numerically stiff, the calculations are not yet precise relic-density predictions. Instead, the two-field result should be interpreted as diagnostic evidence for the qualitative dynamics of coupled glueball dark matter and as motivation for improved numerical treatment.

Populärvetenskaplig sammanfattning

Den materia vi känner till, atomerna som bygger upp planeter, stjärnor, gasmoln och galaxer, utgör bara en liten del av universums totala energiinnehåll. Resten består till största del av mörk materia och mörk energi. Mörk materia är materia som inte kan observeras med ljus, men vars gravitationella påverkan är nödvändig för att förklara hur galaxer roterar, hur galaxhoper hålls samman och hur strukturer i universum har vuxit fram.

I detta arbete undersöks en möjlig förklaring till mörk materia baserad på en så kallad mörk Yang-Mills-teori. Yang-Mills-teorier är gaugeteorier som baseras på symmetrigrupper av typen $SU(N)$. En välkänd sådan Yang-Mills-teori är den $SU(3)$-teori som i standardmodellen beskriver hur den starka kraften binder ihop kvarkar och gluoner till hadroner. Hadroner bildas på grund av att partiklar med färgladdning måste existera som färglösa sammansatta partiklar. En av gluonernas viktiga egenskaper är därmed att de själva bär på färgladdning, vilket gör att de kan interagera med varandra och bilda bundna tillstånd som kallas gluonbollar. En föreslagen mörk Yang-Mills sektor som ger upphov till mörka gluonbollar som endast interagerar svagt med synlig materia är därmed troliga kandidater för mörk materia.

I det tidiga universum var temperaturen så hög att de mörka gluonerna kunde existera som en varm gas. När universum expanderade och därmed kyldes ned genomgick den mörka sektorn en fasövergång där gluonerna bands samman till gluonbollar. I denna uppsats studeras hur ett sådant fält utvecklas kosmologiskt genom fasövergången och hur mycket mörk materia som blir kvar idag. Först behandlas en modell med en skalär gluonboll för gaugegrupperna $SU(3)$, $SU(4)$ och $SU(5)$. Därefter undersöks en mer preliminär två-gluonbollsmodell med både skalära och pseudoskalära frihetsgrader. Den senare delen är utforskande och visar framför allt vilka teoretiska och numeriska problem som måste lösas innan en precis beräkning av reliktätheten kan göras.

Contents

1 Introduction

The particle nature of dark matter remains one of the central open questions in particle physics and cosmology. The existence of dark matter is inferred from gravitational phenomena, including galactic rotation curves, gravitational lensing, the dynamics of galaxy clusters and the formation of large-scale structures. Despite this, no non-gravitational interaction of dark matter with Standard Model particles have been observed, which motivates the study of theoretically well-defined dark sectors that may be very weakly coupled, or coupled only gravitationally, to the visible sector.

One simple and predictive possibility is that dark matter may arise from a pure dark Yang-Mills theory with gauge groups $SU(N)$, where the fundamental degrees of freedom are massless dark gluons. At high temperatures these gluons form a deconfined plasma, and at temperatures of order of the confinement scale Λ they undergo a confinement phase transition [1–4]. After the phase transition, the physical spectrum consists of color-singlet bound states known as glueballs. The lightest scalar glueball, usually denoted 0^{++}, can be stable in a pure Yang-Mills sector and is therefore a natural dark matter candidate.

The cosmological abundance of glueball dark matter is nontrivial to calculate. The relevant dynamics occur near a strongly coupled first-order phase transition, where perturbative methods are not reliable. The single-glueball model used in Refs. [5, 6] addresses this by combining a scalar glueball effective theory with the Polyakov-loop description of the deconfinement order parameter. This makes it possible to follow the field evolution through the phase transition and to extract the relic abundance from the late-time averaged energy density.

The first aim of this thesis is to reproduce the single-glueball calculation for $SU(N)$ gauge groups with $N = 3, 4, 5$. This includes the effective potential, the integration of the non-dynamical Polyakov-loop, the temperature-dependent equation of motion in an expanding radiation-dominated Universe, and the extraction of the relic density.

The second aim is to explore how the analysis changes if one includes both scalar and pseudoscalar glueball degrees of freedom. This is motivated by the composite heavy axion-like particle framework in Ref. [7], where a pseudoscalar glueball can behave as a heavy composite axion-like particle. In contrast to conventional elementary axion-like particles, whose photon coupling is usually controlled by an effective Peccei–Quinn scale, the composite scenario can strongly suppress this coupling through heavy fermion portal effects, $g_{\mathrm{GALP}\gamma} \propto m^3_{\mathrm{GALP}}/M^4_{\Psi}$. The two-glueball part of this thesis should therefore be read as an exploratory step toward such a richer dark-sector phenomenology, not as a complete finite-temperature relic-density calculation.

The thesis is organized as follows, Section 2 reviews the single-glueball Polyakov-loop model and its cosmological evolution. Section 3 introduces the scalar-pseudoscalar two-glueball effective theory and explains its limitations. Section 4 presents the numerical results and discusses which conclusions are robust and which remain preliminary. The appendices collect the derivations of the field equations and the time-temperature relation used in the cosmological evolution.

2 Single Glueball Model

2.1 Effective Potential

As the Universe expands and cools, a pure dark $SU(N)$ gauge sector undergoes a confinement-deconfinement phase transition at a critical temperature T_c. Above T_c, dark gluons exist as a deconfined thermal plasma. Below T_c, the gluons become confined into bound states known as glueballs. Understanding this phase transition is therefore essential for determining how the dark glueballs are generated and for describing their subsequent cosmological evolution.

The confinement-deconfinement phase transition in pure $SU(N)$ gauge theories is non-perturbative and therefore becomes difficult to analyze directly. However, at finite temperature T the center $\mathbb{Z}_N$ of the $SU(N)$ gauge group is a relevant global symmetry [8]. Therefore gauge-invariant operators charged under this symmetry can be constructed, the most notable one being the Polyakov loop. Since the Polyakov loop serves as an order parameter for the deconfinement phase transition, we deploy an effective field theory defined in Ref. [9] to describe the dynamics of the dark glueballs. The Polyakov loop is defined as follows

$$\ell(x) = \frac{1}{N}\mathrm{Tr}\mathcal{P}\mathrm{exp}\left[ig\int_0^{1/T} A_0(\tau, x)d\tau\right], \tag{2.1}$$

where $\mathcal{P}$ denotes path ordering, A_0 is the Euclidean temporal component of the dark gauge field, and g is the $SU(N)$ gauge coupling. The Polyakov loop transforms non-trivially under the center symmetry and its expectation value distinguishes the confined and deconfined phases. Below the critical temperature T_c the Polyakov loop has a global minimum at $\ell = 0$. Above T_c a nonzero minimum, $\ell = \ell_+$, is energetically favoured. The Polyakov Loop Model (PLM) uses this order parameter to describe the Yang-Mills confinement transition in a mean-field approach [10].

The gluon-glueball dynamics is described by the effective potential [9]

$$V(\mathcal{H}, \ell) = \frac{\mathcal{H}}{2}\ln\left[\frac{\mathcal{H}}{\Lambda^4}\right] + T^4\mathcal{V}_N(\ell, T) + \mathcal{H}\mathcal{P}(\ell) + V_T(\mathcal{H}). \tag{2.2}$$

The first term preserves the trace anomaly constraint and describes the potential of the glueball at zero temperature [11, 12], here Λ is the confinement scale. $\mathcal{V}_N(\ell, T)$ and $\mathcal{P}(\ell)$ are real polynomials which are invariant under $\mathbb{Z}_N$ whose constants are fit to lattice data. The $\mathcal{H}\mathcal{P}(\ell)$ term describes the most general interaction term which can be constructed between the glueball field $\mathcal{H}$ and the Polyakov loop ℓ without breaking the zero-temperature trace anomaly [9]. Lastly, the $V_T(\mathcal{H})$ term accounts for thermal corrections, it is omitted from the potential moving forward in accordance with Ref. [5], since its impact on the glueball potential is negligible. In the confined phase, $T \ll T_c$, the potential (2.2) reduces to describe the glueball dynamics. Similarly in the deconfined phase $T \gg T_c$ the PLM term $T^4\mathcal{V}(\ell)$ dominates. The relation between the confinement scale Λ and the critical temperature is set by lattice simulations, here $T_c = (1.59 + 1.22/N^2)\Lambda$ is used for $N = 3, 4, 5$ [5, 13, 14].

The Lagrangian describing the glueball and Polyakov loop degrees of freedom is [9, 15, 16]

$$\mathcal{L} = \frac{c}{2}\frac{\partial_\mu\mathcal{H}\partial^\mu\mathcal{H}}{\mathcal{H}^{3/2}} - V(\mathcal{H}, \ell), \tag{2.3}$$

where, $c = \frac{1}{2\sqrt{e}}(\Lambda/m_{gb})^2$. Here, e refers to Euler's number and the mass of the glueball is $m_{gb} = 6\Lambda$ [17]. In order to canonically normalize the glueball field, it is redefined as ϕ where $\mathcal{H} = 2^{-8}c^{-2}\phi^4$. To rewrite the Lagrangian (2.3), we find the derivatives of the redefined glueball field

$$\partial_\mu \mathcal{H} = \frac{1}{2^8 c^2}\partial_\mu \phi^4 = \frac{\phi^3}{2^6 c^2}\partial_\mu \phi, \tag{2.4}$$

and analogously

$$\partial^\mu \mathcal{H} = \frac{1}{2^8 c^2}\partial^\mu \phi^4 = \frac{\phi^3}{2^6 c^2}\partial^\mu \phi. \tag{2.5}$$

The kinetic term can therefore be written as

$$\mathcal{L}_{kin} = \frac{1}{2}\partial_\mu \phi \partial^\mu \phi, \tag{2.6}$$

which means that the field ϕ is canonically normalized.

To then rewrite the potential (2.2) in terms of ϕ, we see that only the terms which are dependent on $\mathcal{H}$ will be changed, and the redefined potential can therefore be written as

$$\begin{aligned} V(\phi,\ell) &= \frac{1}{2}\frac{\phi^4}{2^8 c^2}\ln\left[\frac{\phi^4}{2^8 c^2 \Lambda^4}\right] + T^4\mathcal{V}_N(\ell,T) + \frac{\phi^4}{2^8 c^2}\mathcal{P}(\ell) + V_T(\mathcal{H}) \\ &= \frac{\phi^4}{2^8 c^2}\left(2\ln\left[\frac{\phi}{\Lambda}\right] - 4\ln 2 - \ln c\right) + T^4\mathcal{V}_N(\ell,T) + \frac{\phi^4}{2^8 c^2}\mathcal{P}(\ell), \end{aligned} \tag{2.7}$$

where $\mathcal{P}(\ell) = c_1|\ell|^2$. In Ref. [5] the value for c_1 was found to be $c_1 = 1.225 \pm 0.19$ at 95% confidence level (CL) for $SU(3)$. The error for $SU(3)$ was then increased with a factor 4 to obtain the value $c_1 = 1.225 \pm 0.8$ which are used for $SU(4)$ and $SU(5)$. As done in Ref. [5], the value has been fixed to $c_1 = 1.225$ to generate all figures for all gauge groups in this paper. In the second line of (2.7), the thermal correction $V_T(\mathcal{H})$ has been neglected, following Refs. [5, 6], since its effect on the glueball potential is negligible compared with the dominant phase-transition dynamics and the uncertainty associated with c_1.

After redefining the glueball field as ϕ, the dynamics is determined by the Lagrangian

$$\mathcal{L} = \frac{1}{2}\partial_\mu \phi \partial^\mu \phi - V(\phi,\ell). \tag{2.8}$$

For a $SU(N)$ group with $N = 3, 4, 5$, the Polyakov loop potential $\mathcal{V}_N(\ell,T)$ preserves the Z_N symmetry and is determined by lattice thermodynamic quantities to be [3]

$$\mathcal{V}_N(\ell,T) = -\frac{b_2(T)}{2}|\ell|^2 - b_3(\ell^N + \ell^{*N}) + b_4|\ell|^4 + b_6|\ell|^6, \tag{2.9}$$

where

$$b_2(T) = a_0 + a_1\left(\frac{T_c}{T}\right) + a_2\left(\frac{T_c}{T}\right)^2 + a_3\left(\frac{T_c}{T}\right)^3 + a_4\left(\frac{T_c}{T}\right)^4. \tag{2.10}$$

The parameters of the potential are shown in Table 2.1.

Table 2.1: Parameters for the Polyakov loop potential [5]

N	3	4	5
a_0	3.72	9.51	14.3
a_1	-5.73	-8.79	-14.2
a_2	8.49	10.1	6.40
a_3	-9.29	-12.2	1.74
a_4	0.27	0.489	-10.1
b_3	2.40	0	-5.61
b_4	4.53	-2.46	-10.5
b_6	0	3.23	0

Using the definitions for $\mathcal{V}_N(\ell, T)$ and $\mathcal{P}(\ell)$, the potential (2.7) can be written as

$$V(\phi, \ell) = A\frac{\phi^4}{2}\ln\left(A\frac{\phi^4}{\Lambda^4}\right) + T^4\left(-\frac{b_2(T)}{2}|\ell|^2 - b_3(\ell^N + \ell^{*N}) + b_4|\ell|^4 + b_6|\ell|^6\right) + A\phi^4 c_1|\ell|^2, \tag{2.11}$$

where $A = \frac{1}{2^8 c^2}$.

The Polyakov loop potential is shown in the left panel of Figure 2.1 for the three different gauge groups in both the deconfined and confined phase. The right panel of Figure 2.1 shows the evolution of the minimum of the Polyakov loop. We can clearly see that since the Polyakov loop is always zero for temperatures lesser than the critical, $\ell = 0$ is a global minimum of the potential. At temperatures above the critical one, we see that there is another minima $\ell = \ell_+$.

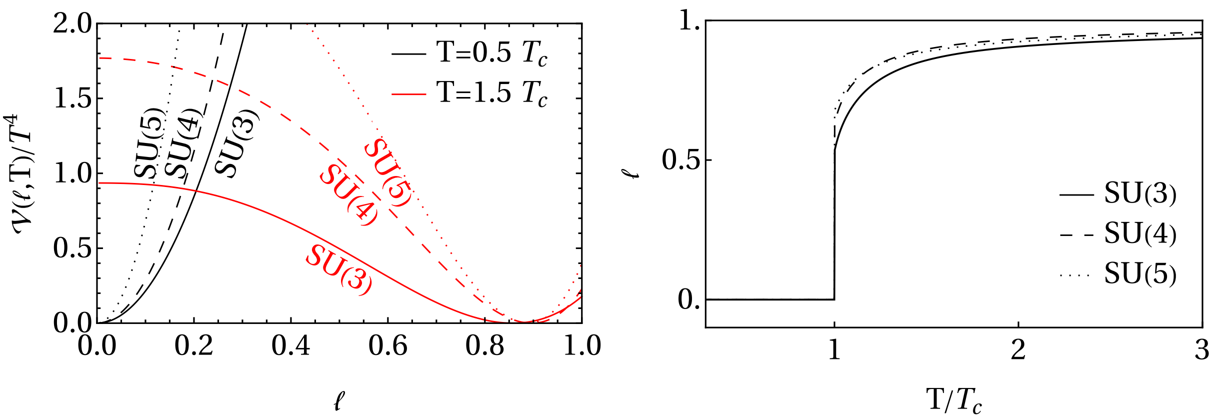

Figure 2.1: *Left:* Polyakov-loop potential $\mathcal{V}_N(\ell, T)$ for $SU(N)$ where $N = 3, 4, 5$. The minimum of the potential has been arbitrarily set to zero. *Right:* Evolution of the Polyakov loop ℓ as a function of temperature. Reproduced following Figure 1 in Ref. [5].

The minima of the Polyakov loop ℓ_+ is found by minimizing the Polyakov loop potential (2.11) in terms of ℓ for each $N = 3, 4, 5$. For $SU(3)$, the non-zero minimum is found to be

$$\ell_+ = \frac{3b_3}{4b_4}\left(1 + \sqrt{1 + \frac{512 b_2(T) b_4 - 4\frac{c_1 b_4}{c^2}\left(\frac{\phi}{T}\right)^4}{1152 b_3^2}}\right), \tag{2.12}$$

and similarly the minima for $SU(4)$ and $SU(5)$ are found by minimizing the potential in terms of ℓ. Since the Polyakov loop is non-zero for temperatures above T_c, $\ell = \ell_+$ becomes the global minimum in the deconfined phase. The Polyakov loop can therefore be integrated out using the minimum $\ell = \ell(\phi, T)$ in order to write the potential on the form $V(\phi, T) = V(\phi, \ell(\phi, T))$. The minimum of this potential is set to zero in order to describe glueballs as matter. The potential is shown in the left panel of Figure 2.2 for $T > T_c$ and $T < T_c$.

The evolution of the re-normalized mass of the glueball field can be calculated as a function of temperature from the second derivative of the potential

$$m_{gb}^2(T) = \left.\frac{\partial^2 V(\phi, T)}{\partial \phi^2}\right|_{\phi=\phi_{min}}, \tag{2.13}$$

which is evaluated at the minimum of the glueball field ϕ_{min} as a function of temperature. The evolution of the glueball mass is shown in the right panel of Figure 2.2. This figures shows that the glueball mass $m_{gb} = 6\Lambda$ is fixed in the confined phase.

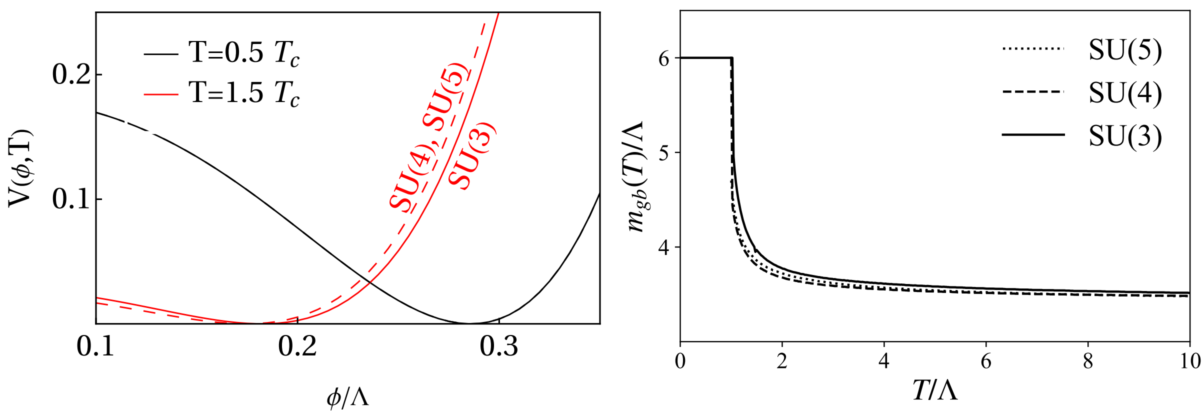

Figure 2.2: *Left:* Glueball potential for $SU(N)$, $N = 3, 4, 5$. The confined phase is shown in black which is not dependent on choice of gauge group. The deconfined phase is in red where SU(3) is the solid line and the dashed line is SU(4) and SU(5). The minima of the potential has been set to zero to describe glueballs as matter. *Right:* Evolution of glueball mass as a function of the temperature for $SU(N)$. Reproduced following Figure 2 in Ref. [5].

2.2 Cosmological evolution

The glueball field is approximated to be spatially homogeneous and evolves in an expanding Friedman-Lemaître-Robertson-Walker (FLRW) Universe. The Klein-Gordon equation (see Appendix A.1 for a detailed derivation) for the field is therefore

$$\ddot{\phi} + 3H\dot{\phi} + \partial_\phi V(\phi, T) = 0, \tag{2.14}$$

where the derivatives are taken with respect to the cosmic time t and the Hubble parameter for a radiation-dominated Universe is $H = 1/(2t)$, assuming an approximately constant number of relativistic degrees of freedom. The associated energy density and pressure to the scalar field ϕ is

$$\rho = \frac{1}{2}\dot{\phi}^2 + V(\phi, T), \qquad p = \frac{1}{2}\dot{\phi}^2 - V(\phi, T). \tag{2.15}$$

These quantities should not be interpreted as the total energy density and pressure of the full dark sector, but instead describe the glueball excitations above the subtracted thermal and vacuum background contributions. The equation of state, $w = p/\rho$, is then the ratio of pressure and energy density. The equation of state is a useful diagnostic, since after the phase transition, the potential can temporarily produce $p \neq 0$. However, at sufficiently low temperature the field oscillates around an approximately quadratic minimum and behaves as cold dark matter.

Since the phase transition is expected to happen during a radiation-dominated era, there is a relation between time t and the photon temperature T_γ (see Appendix B for a derivation of the relation),

$$t = \frac{1}{2}\sqrt{\frac{45}{4\pi^3 g_{*,\rho}(T_\gamma)}}\frac{m_P}{T_\gamma^2}, \tag{2.16}$$

where m_P is the Planck mass and $g_{*,\rho}(T_\gamma)$ is the number of degrees of freedom in the SM bath at $T_\gamma = \zeta_T T$. Here, ζ_T is determined by the interactions with the visible sector and is therefore model dependent. This expression for the cosmic time can be used to rewrite the equation of motion for ϕ, (2.14), as a function of temperature (see Appendix C for details). The equation of motion of the glueball field as a function of T is

$$\frac{4\pi^3 g_{*,\rho}(T_\gamma)}{45 m_P^2}\zeta_T^4 T^6 \frac{\mathrm{d}^2\phi}{\mathrm{d}T^2} + \frac{2\pi^3}{45 m_P^2}\frac{\mathrm{d}g_{*,\rho}(T_\gamma)}{\mathrm{d}T}\zeta_T^4 T^6 \frac{\mathrm{d}\phi}{\mathrm{d}T} + \frac{\partial V(\phi, T)}{\partial \phi} = 0 \tag{2.17}$$

By neglecting the $\mathrm{d}g_{*,\rho}(T_\gamma)/\mathrm{d}T$ term when $g_{*,\rho}(T_\gamma)$ is approximately constant, this is simplified to be

$$\mu^2 \tilde{T}^6 \frac{\mathrm{d}^2\tilde{\phi}}{\mathrm{d}\tilde{T}^2} + \partial_{\tilde{\phi}} \tilde{V}(\tilde{\phi}, \tilde{T}) = 0, \tag{2.18}$$

where $\mu^2 = \frac{4\pi^3 g_{*,\rho}\zeta_T^4}{45}\left(\frac{\Lambda}{m_P}\right)^2$, $\tilde{\phi} = \phi/\Lambda$, $\tilde{T} = T/\Lambda$ and $\tilde{V} = V/\Lambda^4$.

Similarly the energy density and pressure is simplified to be

$$\tilde{\rho} = \frac{\mu^2 \tilde{T}^6}{2}\left(\frac{\mathrm{d}\tilde{\phi}}{\mathrm{d}\tilde{T}}\right)^2 + \tilde{V}(\tilde{\phi}, \tilde{T}), \tag{2.19}$$

and

$$\tilde{p} = \frac{\mu^2 \tilde{T}^6}{2}\left(\frac{\mathrm{d}\tilde{\phi}}{\mathrm{d}\tilde{T}}\right)^2 - \tilde{V}(\tilde{\phi}, \tilde{T}). \tag{2.20}$$

In order to obtain the cosmological evolution of the glueball field, (2.18) is solved numerically using `Mathematica`'s `NDSolve` routine. The evolution is performed starting at a high-temperature initial point $\tilde{T}_i > \tilde{T}_c$ down to a final point $\tilde{T}_f < \tilde{T}_c$. The solution is shown in Figure 2.3. At the first-order confinement transition, the minimum of the effective potential changes discontinuously. The glueball field is then displaced from the new confined-phase minimum and begins to oscillate around it. At sufficiently low temperature, these oscillations occur in an approximately quadratic potential and the averaged energy density redshifts as cold dark matter.

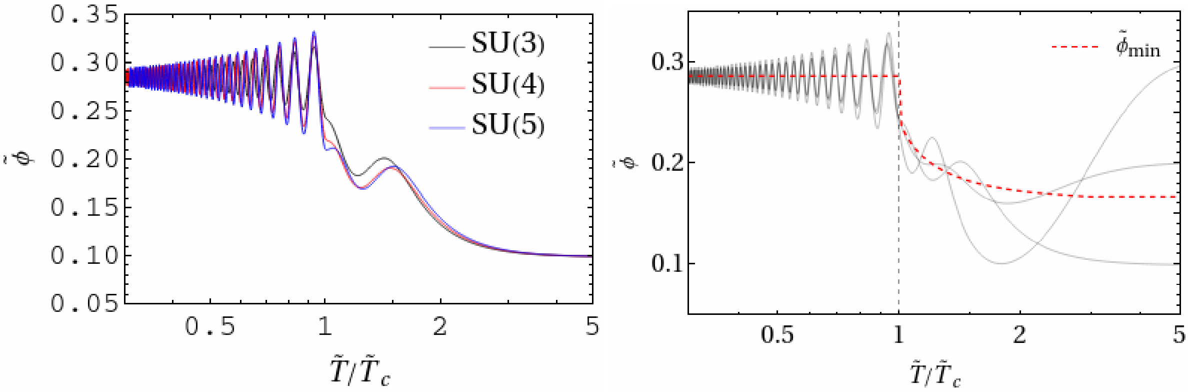

Figure 2.3: *Left:* Evolution of the glueball field by solving to (2.18) using initial conditions $\tilde{\phi}(\tilde{T}_i) = 0.1$, $\frac{d\tilde{\phi}}{d\tilde{T}}|_{\tilde{T}=\tilde{T}_i} = 0.1$ and $\mu = 0.05$. *Right:* Evolution of glueball field for SU(3) for two additional initial conditions. The red dashed line shows the evolution of the minima of the glueball field. The initial condition used are chosen to reproduce the results from Figure 3 in Figure 3 in Ref. [5]

The energy density and pressure were evolved using the solutions obtained for the field by evolving (2.19) and (2.20), the evolution of the energy density and pressure is presented in Figure 2.4.

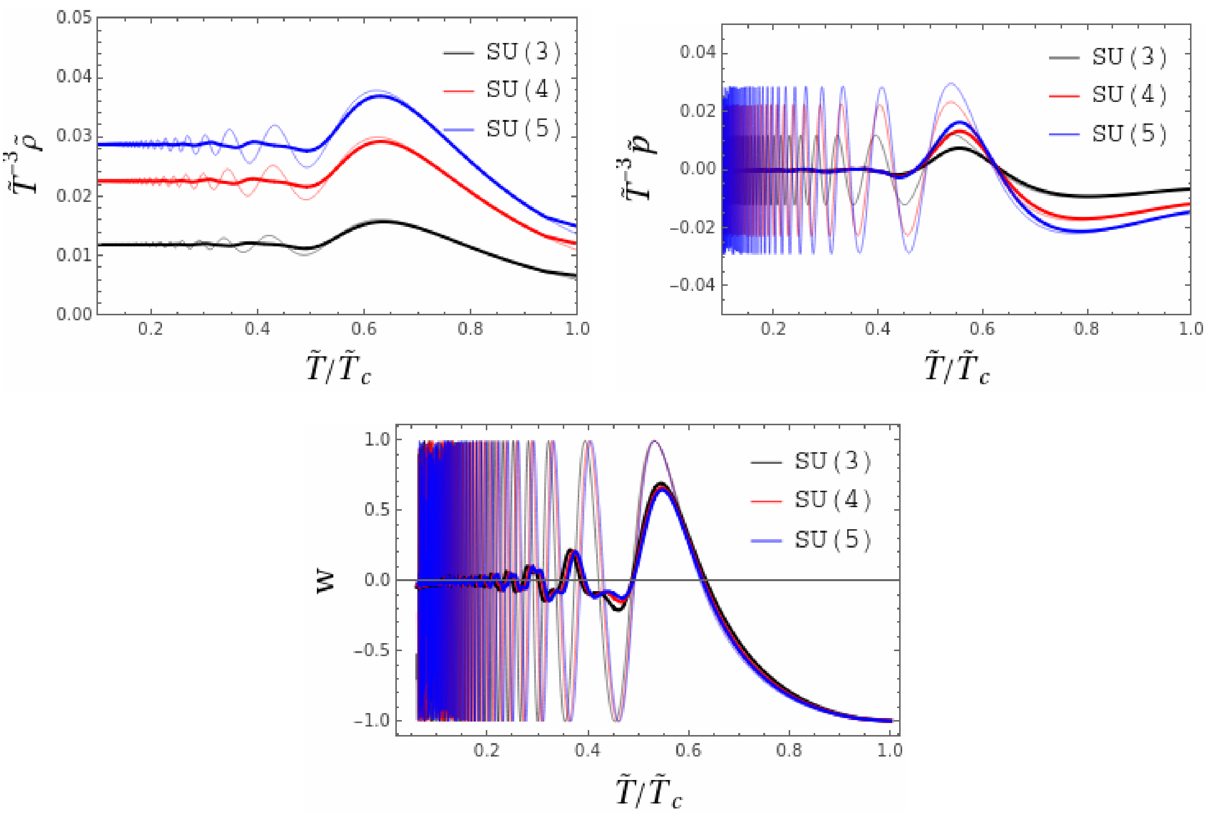

Figure 2.4: *Top:* Evolution of the energy density found by solving (2.19) (left) and pressure by solving (2.20) (right) using $\mu = 1$. The opaque lines shows the evolution averaged over the dynamical period. *Bottom:* Evolution of the equation of state $w = p/\rho$, the opaque lines shows the evolution averaged over the dynamical period. Adapted from Figure 4 in Ref. [5].

2.3 Relic density

As seen in Figure 2.4, the energy density (2.19) is oscillating. Therefore, ρ is averaged during the last oscillation before $\tilde{T}_f$ as follows [5]

$$\left\langle \frac{\tilde{\rho}}{\tilde{T}^3} \right\rangle_f = \frac{1}{0.3\tilde{T}_f} \int_{\tilde{T}_f}^{1.3\tilde{T}_f} \frac{\tilde{\rho}(\tau)}{\tau^3} \mathrm{d}\tau. \tag{2.21}$$

Once the averaged quantity has saturated, it becomes independent of the overall confinement scale, while the final relic abundance scales linearly with Λ. In order to calculate the relic density of glueballs today, the energy density (2.21) is diluted with the factor $(T_{\gamma,0}/\zeta_T T_f)^3$ which takes the expansion of the Universe into account. The density therefore becomes

$$h^2\Omega_g = \frac{\Lambda}{\rho_c/h^2} \left\langle \frac{\tilde{\rho}}{\tilde{T}^3} \right\rangle_f T_f^3 \left(\frac{T_{\gamma,0}}{\zeta_T T_f} \right)^3 = 0.12\zeta_T^{-3} \frac{\Lambda}{\Lambda_0}. \tag{2.22}$$

Here, the critical density is $\rho_c/h^2 = 1.05 \times 10^4$ eVcm^{-3}, the scaling factor for the Hubble expansion is $h = 0.674$ and $T_{\gamma,0} = 0.235$ meV is the temperature of the photon bath today [18]. As in [5], Λ_0 is defined as the phase transition scale which makes glueballs make up the totality of DM. The parameter ζ_T, which is related to the glueball and photon temperatures, is used instead of ζ_T' which also depends on the degrees of freedom in the Universe. Therefore Refs. [5, 6] found that the dependence on μ is weak in the case where $\mu \ll 1$, which is the case for phase transition scales far below the Planck scale. By using this approximation, the relic density is predicted with an error of less than $\sim 10\%$ [5].

3 Two Glueball Model

The single-scalar glueball model used in Section 2 considers only the lightest scalar 0^{++} glueball degrees of freedom. A more complete pure Yang-Mills spectrum also includes the lightest pseudoscalar glueball channel, denoted 0^{-+}. This motivates an exploratory two-glueball effective theory containing a scalar and pseudoscalar field. The purpose of this section is not to construct a fully lattice-calibrated finite-temperature two-field phase-transition model. Instead, we formulate a controlled benchmark which illustrates how coupled scalar and pseudoscalar glueball fields may evolve through the confinement transition.

The scalar field h denotes the canonically normalized 0^{++} degrees of freedom, while a denotes the canonically normalized 0^{-+} pseudoscalar degrees of freedom. The two fields are defined as [7]

$$h^4 \equiv -\frac{\beta(g)}{2g} G^a_{\mu\nu} G^{\mu\nu a}, \quad ah^3 \equiv G^a_{\mu\nu} \tilde{G}^{\mu\nu a}, \tag{3.1}$$

in terms of gauge invariant operators of the lowest dimension and the β-function $\beta(g)$. From these definition, we see that both fields h and a have mass dimension one. The dynamics of these fields are determined by the corresponding low-energy composite EFT Lagrangian [11, 19]

$$\mathcal{L} = \frac{1}{2}\partial_\mu h \partial^\mu h + \frac{1}{2}\partial_\mu a \partial^\mu a - V_{\text{eff}}(h, a). \tag{3.2}$$

The trace anomaly constrains the effective potential to the following form [7]

$$V_{\text{eff}} \simeq c_0 h^4 \ln\left(\frac{h}{\Lambda}\right) + \frac{\theta}{4} a h^3 + h^4 f\left(\frac{a}{h}\right) + c_1 h^4 + c_2 h^2 a^2 + c_3 a^4 + c_4 h a^3. \tag{3.3}$$

Here θ and the coefficients c_i are non-perturbative parameters which should ultimately be fixed by lattice simulations, while f is an arbitrary continuous function which we put to zero moving forward.

At zero temperature we impose a CP-conserving vacuum

$$h(T=0) = h_0, \quad a(T=0) = a_0 = 0, \tag{3.4}$$

and we set the zero-temperature CP-violating parameter to zero

$$\theta = 0. \tag{3.5}$$

Therefore the scalar and pseudoscalar fields do not mix at $T = 0$, so the zero-temperature mass eigenstates coincide with the definite-parity glueball states. This justifies using the lattice-motivated values in the confined phase [17]

$$m_{0^{++}} = 6\Lambda, \quad m_{0^{-+}} = 9\Lambda. \tag{3.6}$$

In this CP-conserving vacuum the physical low-temperature fluctuations are simply

$$\phi_h = h - h_0, \quad \phi_a = a. \tag{3.7}$$

The scalar part of the potential is chosen to reproduce the one-glueball logarithmic potential used in Section 2. The two-field zero-temperature potential used in the benchmark is

$$V_0(h,a) = \frac{h^4}{2^8 c^2}\left(2\ln\left(\frac{h}{\Lambda}\right) - 4\ln 2 - \ln c\right) + \frac{1}{2e} + c_2 h^2 a^2 + c_3 a^4 + c_4 h a^3. \tag{3.8}$$

The parameters c and c_2 are fixed by requiring that $(h_0, 0)$ is a stationary point and that the Hessian at this point reproduces the physical masses $m_{0^{++}}$ and $m_{0^{-+}}$. The parameters c_3 and c_4 are treated as benchmark interaction parameters. The term $c_4 h a^3$ is odd under $a \to -a$ and therefore represents a CP-odd deformation of the thermal effective theory. In the present benchmark CP is nevertheless restored in the zero-temperature vacuum because $a_0 = 0$ and the Hessian has no scalar–pseudoscalar mixing at this point. The zero-temperature matching conditions are

$$\left.\frac{\partial V_0}{\partial h}\right|_{(h_0,0)} = 0, \qquad \left.\frac{\partial V_0}{\partial a}\right|_{(h_0,0)} = 0, \tag{3.9}$$

$$\left.\frac{\partial^2 V_0}{\partial h^2}\right|_{(h_0,0)} = m_{0^{++}}^2, \qquad \left.\frac{\partial^2 V_0}{\partial a^2}\right|_{(h_0,0)} = m_{0^{-+}}^2, \qquad \left.\frac{\partial^2 V_0}{\partial h \partial a}\right|_{(h_0,0)} = 0. \tag{3.10}$$

For the logarithmic normalization used here these conditions give

$$\frac{h_0}{\Lambda} = \frac{2\sqrt{2/e}}{m_{0^{++}}/\Lambda}, \qquad c = \frac{\sqrt{e}\, h_0^2}{16} \tag{3.11}$$

and the coefficient c_2 is fixed by the pseudoscalar mass condition. The remaining parameters c_3 and c_4 are not yet known from lattice simulations and are therefore varied as benchmarks. At finite temperature the scalar glueball couples to the Polyakov loop in the same way as in the single-glueball model. The finite-temperature potential is

$$V_T(h,a,\ell) = V_0(h,a) + T^4 \mathcal{V}_N(\ell,T) + \frac{c_1 h^4}{2^8 c^2}|\ell|^2, \tag{3.12}$$

where $\mathcal{V}_N(\ell,T)$ is the Polyakov-loop potential introduced in Eq. (2.11), and $c_1 = 1.225$ is the same lattice-motivated coupling used in the single-glueball model. The Polyakov loop is treated as a non-dynamical order parameter and is integrated out by minimizing the potential with respect to ℓ,

$$\ell = \ell_\star(h,T), \qquad V_{\text{eff}}(h,a,T) = V_T(h,a,\ell_\star(h,T)). \tag{3.13}$$

The scalar field h directly affects the Polyakov-loop sector, while the pseudoscalar field a enters through the two-field glueball potential and its interactions with h.

As discussed before, in the confined phase the lattice motivated glueball masses $m_{0^{++}} = 6\Lambda$ and $m_{0^{-+}} = 9\Lambda$ are used. Analogously to the single glueball model, the potential is used to find the glueball mass in the deconfined phase as in (3.10) and the evolution of the glueball masses can be seen in Figure 3.1. We see that the lower curve, corresponding to the scalar field h, is the same as the mass evolution for the single-scalar field ϕ as seen in Figure 2.2.

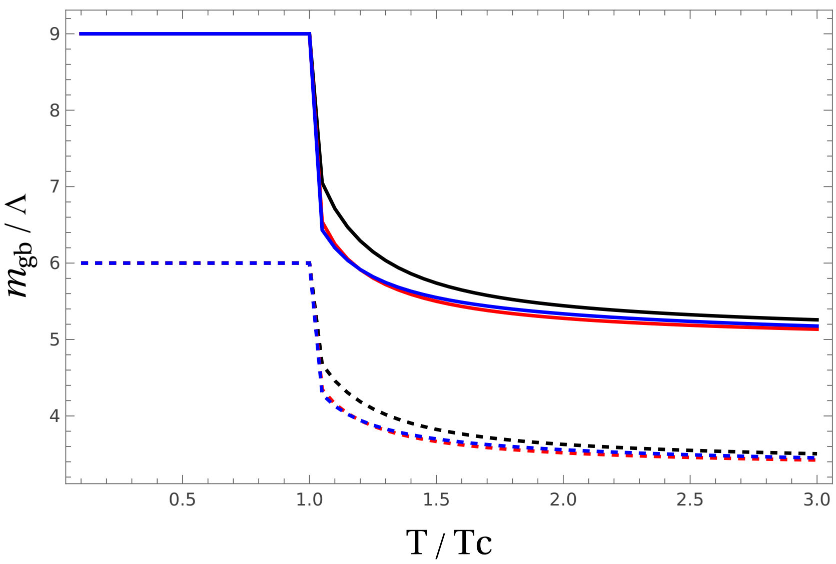

Figure 3.1: Evolution of glueball-mass for the two-field model as a function of temperature. The upper solid lines refer to the pseudoscalar glueball while the lower dashed lines refer to the scalar glueball.

3.1 Cosmological Evolution

The Klein-Gordon equations, as well as the energy density and pressure for the two glueball fields h and a are derived analogously to the equations obtained for the single-glueball model and are outlined in Appendix A.2.

For the two fields we find the coupled equations

$$\ddot{h} + 3H\dot{h} + \frac{\partial V_{\text{eff}}(h, a, T)}{\partial h} = 0, \tag{3.14}$$

$$\ddot{a} + 3H\dot{a} + \frac{\partial V_{\text{eff}}(h, a, T)}{\partial a} = 0. \tag{3.15}$$

The corresponding energy density and pressure is then

$$\rho = \frac{1}{2}\dot{h}^2 + \frac{1}{2}\dot{a}^2 + V_{\text{eff}}(h, a, T), \tag{3.16}$$

$$p = \frac{1}{2}\dot{h}^2 + \frac{1}{2}\dot{a}^2 - V_{\text{eff}}(h, a, T). \tag{3.17}$$

Using the same method as for the single-glueball model as outlined in Appendix C, the Klein-Gordon equations, as well as the energy density and pressure, are rewritten using the relation between time and photon temperature to be dependent only on time. The equations are therefore read

$$\mu^2\tilde{T}^6\frac{\mathrm{d}^2\tilde{h}}{\mathrm{d}\tilde{T}^2} + \frac{\partial V(\tilde{h}, \tilde{a}, \tilde{T})}{\partial \tilde{h}} = 0, \quad \mu^2\tilde{T}^6\frac{\mathrm{d}^2\tilde{a}}{\mathrm{d}\tilde{T}^2} + \frac{\partial V(\tilde{h}, \tilde{a}, \tilde{T})}{\partial \tilde{a}} = 0 \tag{3.18}$$

$$\tilde{\rho} = \frac{\mu^2\tilde{T}^6}{2}\left(\left(\frac{\mathrm{d}\tilde{h}}{\mathrm{d}\tilde{T}}\right)^2 + \left(\frac{\mathrm{d}\tilde{a}}{\mathrm{d}\tilde{T}}\right)^2\right) + \tilde{V}(\tilde{h}, \tilde{a}, \tilde{T}), \quad \tilde{p} = \frac{\mu^2\tilde{T}^6}{2}\left(\left(\frac{\mathrm{d}\tilde{h}}{\mathrm{d}\tilde{T}}\right)^2 + \left(\frac{\mathrm{d}\tilde{a}}{\mathrm{d}\tilde{T}}\right)^2\right) - \tilde{V}(\tilde{h}, \tilde{a}, \tilde{T}) \tag{3.19}$$

As before, tilded quantities denote dimensionless variables obtained by rescaling all dimensionful quantities with the confinement scale Λ.

4 Results and Discussion

4.1 Single Glueball Relic Abundance

The results from the single-glueball model are presented in Table 4.1. In the second column we see that the central value $c_1 = 1.225$ is used for all gauge groups, and only the assigned uncertainty differs. In the third column we see the calculated values obtained from (2.21) and the energy scale Λ_0 in the fourth column. We also see that our calculated values are in agreement with the results presented in [5] for each gauge group.

Table 4.1: Results from the calculation of the relic abundance of glueballs. The values shown in the third column are obtained by computing the integral in (2.21) using `Mathematica`'s `NIntegrate` function with the energy density $\tilde{\rho}$ as defined in (2.21) which in turn comes from the solution of the cosmological evolution (2.18). The results are obtained using $\mu = 0.001$ and $\tilde{T}_f = 0.1$. The values in the third column can then be used to calculate the relic density using (2.22) and to calculate the energy scale Λ_0 which is seen in the last column.

N	c_1	$100 \times \left\langle \frac{\tilde{\rho}}{\tilde{T}^3} \right\rangle_f$	Λ_0 (eV)
3	1.225 ± 0.19	0.595	125
4	1.225 ± 0.8	1.08	68.9
5	1.225 ± 0.8	1.36	54.7

As stated in [5], the relic densities obtained in this framework are significantly smaller than several earlier estimates in the literature, typically by about one order of magnitude in the original $SU(3)$ comparison and up to one or two orders depending on the assumptions used in previous works (see for example the results found in [13, 20, 21]). Part of the reason for this is because of the potential used. In the confined phase, the glueball potential is expanded around the minimum $\tilde{\phi}_{min} = 4e^{-1/4}\sqrt{c}$ and reads as follows

$$\begin{aligned} \tilde{V}(\tilde{\phi}) &= \frac{\tilde{\phi}^4}{2^8 c^2}(2\ln\tilde{\phi} - 4\ln 2 - \ln c) + \frac{1}{2e} \\ &\simeq \frac{1}{4ce^{1/2}}\delta\tilde{\phi}^2 + \frac{5}{48c^{3/2}e^{1/4}}\delta\tilde{\phi}^3 + \frac{11}{768c^2}\delta\tilde{\phi}^4 + \frac{e^{1/4}}{2560c^{5/2}}\delta\tilde{\phi}^5 + ..., \end{aligned} \tag{4.1}$$

where $\delta\tilde{\phi} = \tilde{\phi} - \tilde{\phi}_{min}$. Note that the original potential used is always valid, while the expanded one is valid only for small perturbations about the minimum $\delta\tilde{\phi} \ll 1$. In this perturbative expansion the potential contains cubic, quartic and higher order interactions. Although the relic abundance ultimately is controlled by number-changing processes such as $3 \to 2$, these do not need to arise only from a local ϕ^5 vertex. They can also be generated by combinations of cubic and quartic interactions. In the literature, it is often considered that glueballs interact only through the $\tilde{\phi}^5$ interaction, but here we consider the lower terms in the potential as well. Figure 4.1 shows the two ways the glueballs can annihilate, we see that both interactions are a $3 \to 2$ number changing annihilation. If one only considers the ϕ^5 interaction, the glueballs can only annihilate through the right mode, which would then suppress the number of interactions.

4.2 Two Glueball model

4.2.1 Cosmological Evolution and Observables

Since the non-perturbative parameters used in the two-glueball finite-temperature effective theory are not yet fixed by lattice simulations, the following results should be understood as benchmark studies. The zero-temperature vacuum is chosen to be CP-conserving, with

$$a_0 = 0, \quad \theta = 0, \quad \alpha = 0, \tag{4.2}$$

so that the states at $T = 0$ can be identified with the lattice inspired 0^{++} and 0^{-+} glueball masses. For the plots in this section the benchmark parameters used are

$$c_3 = 0.3, \quad c_4 = 0.6. \tag{4.3}$$

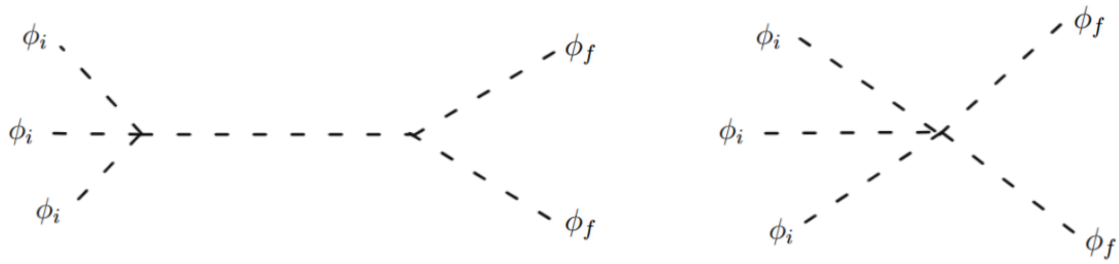

Figure 4.1: *Left:* Feynman diagram showing the $3 \to 2$ process involving a combination of ϕ^3 and ϕ^4 vertices. *Right:* Feynman diagram showing the $3 \to 2$ process involving only the ϕ^5 interaction.

The evolution is obtained by solving the coupled equations (3.14) and (3.15), and the solutions are seen in the left panel of Figure 4.2. Above the phase transition, the scalar field $h(T)$ follows the thermal minimum of the Polyakov-loop-improved potential. At the phase transition, the relevant minimum changes to the confined branch, after which the fields oscillate around the zero temperature vacuum $(h_0, 0)$. This is also seen in the right panel of Figure 4.2 which shows how the scalar field starts to oscillate around its minimum after the confinement phase transition.

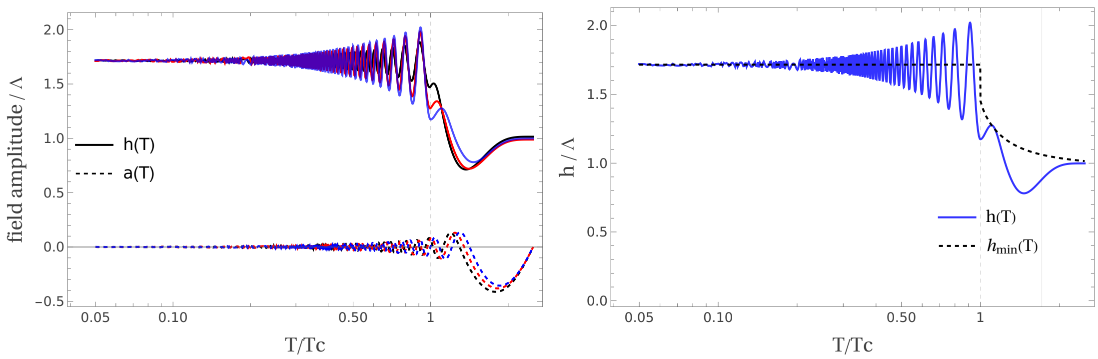

Figure 4.2: *Left*: Cosmological evolution of the scalar $h(T)$ and pseudoscalar $a(T)$ glueball fields in the two-glueball benchmark. The scalar field approaches the confined vacuum value h_0, while the pseudoscalar field evolves around the CP-conserving vacuum value $a_0 = 0$. *Right:* Cosmological evolution of the scalar field along with its minimum for $SU(3)$. The benchmark uses the parameters $m_{0^{++}} = 6\Lambda$, $m_{0^{-+}} = 9\Lambda$, $a_0 = 0$, $\theta = 0$, $\alpha = 0$, $c_3 = 0.3$, $c_4 = 0.6$ as well as the initial conditions $h(T_i) = a(T_i) = 0$ and $\dot{h}(T_i) = \dot{a}(T_i) = 0$.

As seen when comparing the evolution of the two fields at the top of Figure 4.2 to that of the single field in Figure 2.3, the evolution of the scalar field $h(T)$ is most analogous with the results obtained in the single glueball case. In comparison, we see that the pseudoscalar field is excited through its interactions with h. Because the benchmark contains a nonzero c_4 interaction, the finite-temperature trajectory does not need to be symmetric under $a \to -a$, even though the zero-temperature vacuum is CP conserving with $a_0 = 0$. As seen in the right panel of Figure 4.2, the pseudoscalar field can be displaced from zero during the evolution and start oscillating around zero, like how the scalar field oscillates around its minimum. This provides a simple diagnostic example of how CP-odd finite-temperature dynamics could arise during the thermal evolution even though the system ultimately approaches a CP-conserving vacuum at late times.

The evolution of the energy density, pressure and equation of state for the two-glueball model are shown in Figure 4.3. The corresponding single-glueball evolution is also presented using the same parameters as a reference. These observables are more sensitive to the numerical treatment than the fields themselves, because they depend on kinetic terms, the potential normalization and the subtraction of the thermal vacuum energy. They should therefore be interpreted as qualitative diagnostics of the benchmark evolution, not as precision thermodynamic predictions.

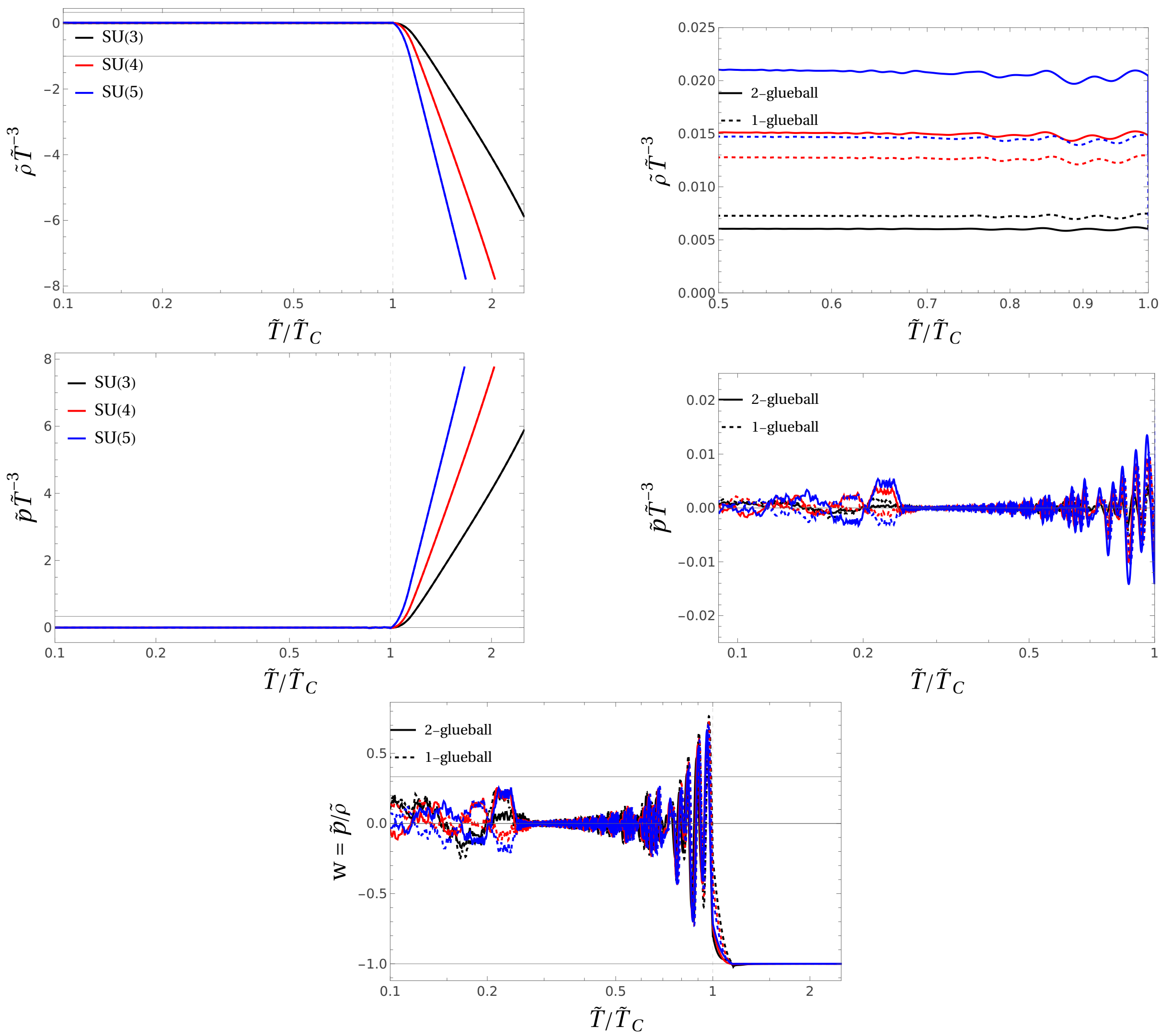

Figure 4.3: Diagnostic thermodynamic observables for the two-glueball benchmark, and corresponding single-glueball observables as a reference. Solid lines refer to the two-glueball model and dashed lines to the single glueball model. $SU(3)$ is shown in black, $SU(4)$ in red and $SU(5)$ in blue in all figures. *Top*: Evolution of the energy-density for the coupled scalar-pseudoscalar fields. The right side shows a zoomed in version to better show the dynamics after the phase transition. *Middle*: corresponding pressure, the right side is also zoomed in to better show the dynamics after the phase transition *Bottom*: Equation-of-state, $w = p/\rho$. The benchmark uses $c_3 = 0.3$, $c_4 = 0.6$, $\mu = 0.01$ and the same initial conditions as Figure 4.2.

4.2.2 Diagnostic Relic Abundance Estimate

The results from the two glueball model are presented in Table 4.2. We see that for these parameter choices, the calculated results are close in scale to the results obtained for the single-glueball model. However, again note that these results are not precision predictions, but primitive diagnostics.

Table 4.2: Diagnostic estimates for the two-glueball benchmark. For all $SU(N)$, the benchmark parameters used were $c_3 = 0.3$, $c_4 = 0.6$, $\mu = 0.01$, and $T_i = 2.5T_c$, $T_f = 0.05T_c$. The values shown in the third column can be used to predict the relic density using (2.22), and they are used to calculate the energy scale Λ_0 shown in the forth column.

N	c_1	$100 \times \left\langle \frac{\tilde{\rho}}{T^3} \right\rangle_f$	Λ_0 (eV)
3	1.225 ± 0.19	0.606	123
4	1.225 ± 0.8	1.52	49
5	1.225 ± 0.8	2.12	35

4.3 Conclusion and Outlook

In this thesis, the cosmological evolution of dark Yang-Mills sectors have been studied using effective glueball descriptions. First, the single-scalar-glueball model was reviewed for $SU(N)$ gauge groups with $N = 3, 4, 5$. The scalar glueball was coupled to the Polyakov loop in order to model the confinement transition, and the subsequent evolution of the field, energy density and pressure was used to estimate the relic abundance. The single-glueball calculation reproduces the qualitative behaviour found in previous studies and illustrates how glueball dark matter can account for the observed abundance for suitable confinement scales.

The model was then extended to an exploratory two-glueball benchmark containing scalar and pseudoscalar glueball degrees of freedom. The benchmark used in this thesis has a CP-conserving zero-temperature vacuum, $a_0 = 0$, $\theta = 0$ and no scalar-pseudoscalar mixing at $T = 0$. This allows the zero-temperature fields to be identified with the lattice-inspired 0^{++} and 0^{-+} glueball states. At finite temperature, the benchmark may include a non-zero $c_4 ha^3$ interaction, which can induce a CP odd thermal dynamics even though the late-time vacuum remains CP conserving.

In both models used here, a key aspect is the subtraction of the temperature-dependent minimum of the effective potential when computing thermodynamic quantities. The subtraction removes the background contribution and isolates the energy density and pressure associated with the glueball excitations. Consequently, the thermodynamic quantities presented in this thesis describe the contributions of the massive glueballs described by the effective field theory, not the quantities of the entire dark sector.

The two-glueball results should be regarded as qualitative diagnostics rather then precision relic-density predictions. The finite-temperature two-field potential is not yet calibrated by lattice simulations, and the late-time oscillatory regime is numerically stiff. Future work should therefore focus on three improvements. First, the two-field potential and its vacuum-energy normalization should be fixed consistently, preferably with lattice input. Second, the numerical evolution should be stabilized so that the evolution of the fields can be followed into lower temperatures, meaning into late-time oscillatory regime where $\tilde{\rho}/\tilde{T}^3$ reaches a plateau. Third, the connection to composite heavy axion-like phenomenology should be developed further, including the role of finite-temperature CP-odd dynamics and the portal-induced coupling to photons. These steps are necessary before the two-glueball framework can be used for a quantitatively reliable relic-density prediction.

Acknowledgments

Firstly I want to thank my supervisor Roman Pasechnik for constant help, guidance and patience during the course of my project. Secondly I also want to thank my friends Bianca, Elise, Ella, Sofie, Lux and Sofia, who have helped me during the project, during the time it took to get here, or both.

A Equation of Motion

A.1 Single Glueball

The covariant action for a scalar field with a temperature dependent potential which interacts with a gravitational field is

$$S = \int \mathcal{L}(\phi, \partial_\mu \phi) \mathrm{d}^4 x = \int \mathcal{L}_{\lceil\rfloor} \sqrt{-g} \mathrm{d}^4 x = \int \left[\frac{1}{2} g^{\mu\nu} \partial_\mu \phi \partial_\nu \phi - V(\phi, T) \right] \sqrt{-g} \mathrm{d}^4 x, \tag{A.1}$$

where the invariant four-volume is $\sqrt{-g}\mathrm{d}^4 x \equiv \sqrt{\det(g_{\mu\nu})}$. The equation of motion then follows from the Euler-Lagrange equation

$$\frac{\partial \mathcal{L}}{\partial \phi} - \partial_\mu \left(\frac{\partial \mathcal{L}}{\partial(\partial_\mu \phi)} \right) = 0. \tag{A.2}$$

Here the first term is

$$\frac{\partial \mathcal{L}}{\partial \phi} = -\sqrt{-g} \frac{\partial V(\phi, T)}{\partial \phi}, \tag{A.3}$$

and the second term is

$$\partial_\mu \left(\frac{\partial \mathcal{L}}{\partial(\partial_\mu \phi)} \right) = -\partial_\mu (\sqrt{-g} g_{\mu\nu} \partial_\nu \phi). \tag{A.4}$$

This means that the Euler-Lagrange equation can be written as

$$\frac{\partial V(\phi, T)}{\partial \phi} = -\frac{1}{\sqrt{-g}} \partial_\mu (\sqrt{-g} g_{\mu\nu} \partial_\nu \phi). \tag{A.5}$$

Then we assume that the scalar field is homogeneous in space and that it evolves according to the FLRW metric such that

$$g_{00} = 1, \qquad g_{ij} = -a^2(t) \delta_{ij}, \tag{A.6}$$

and

$$g^{00} = 1, \quad g^{ij} = -\frac{1}{a^2(t)} \delta_{ij}, \quad \sqrt{-g} = a^3 \tag{A.7}$$

where $a(t)$ is a scale factor as a function of the cosmic time. The equation (A.5) can therefore be expressed

$$\begin{aligned}
\frac{\partial V(\phi, T)}{\partial \phi} &= -\frac{1}{\sqrt{-g}} \partial_\mu (\sqrt{-g} g^{\mu\nu} \partial_\nu \phi) \\
&= -\frac{1}{a^3} \partial_\mu (a^3 (g^{\mu 0} \partial_0 \phi + g^{\mu i} \partial_i \phi)) \\
&= -\frac{1}{a^3} \left(\partial_0 g^{00} (a^3 \partial_0 \phi) + \partial_i g^{0i} (a^3 \partial_0 \phi) \right) \\
&= -\frac{1}{a^3} \frac{\mathrm{d}}{\mathrm{d}t} \left(a^3 \dot{\phi} \right) \\
&= -\frac{1}{a^3} (a^3 \ddot{\phi} + 3a^2 \dot{a} \dot{\phi}) \\
&= -\ddot{\phi} - 3\frac{\dot{a}}{a} \dot{\phi}.
\end{aligned} \tag{A.8}$$

Here we have used $\partial_i \phi = 0$ which comes from the assumption that the scalar field is homogeneous in space. By introducing the Hubble parameter $H = \dot{a}(t)/a(t)$ we find the equation of motion for the glueball field ϕ

$$\ddot{\phi} + 3H\dot{\phi} + \frac{\partial V(\phi, T)}{\partial \phi} = 0 \tag{A.9}$$

In order to derive the equations for the energy density and pressure, we use the fact that the energy-momentum tensor of a scalar field ϕ is

$$T_{\mu\nu} = \partial_\mu \phi \partial_\nu \phi - g_{\mu\nu}\mathcal{L}, \tag{A.10}$$

again we assume spatial homogeneity, the field depends only on time $\phi = \phi(t)$ such that $\partial_i \phi = 0$. Therefore the kinetic term becomes

$$\partial_\mu \phi \partial^\mu \phi = \dot{\phi}^2, \tag{A.11}$$

and the Lagrangian simplifies to

$$\mathcal{L} = \frac{1}{2}\dot{\phi}^2 - V(\phi, T). \tag{A.12}$$

Since the (00) component of the energy-momentum tensor gives the energy density we find from (A.10) and $g_{00} = 1$

$$\rho = \dot{\phi}^2 - \left(\frac{1}{2}\dot{\phi}^2 - V(\phi, T)\right) = \frac{1}{2}\dot{\phi}^2 + V(\phi, T). \tag{A.13}$$

The pressure then comes the spatial part of the energy momentum tensor, and since $\partial_i \phi = 0$, the first term in (A.10) vanishes for all spatial components, leaving

$$p = \mathcal{L} = \frac{1}{2}\dot{\phi}^2 - V(\phi, T). \tag{A.14}$$

A.2 Two Glueball

As in the single glueball derivation, the covariant action for two scalar fields with a temperature dependent potential is

$$S = \int \mathcal{L}\sqrt{-g}\mathrm{d}^4x = \int \left[\frac{1}{2}g^{\mu\nu}\partial_\mu h \partial_\nu h + \frac{1}{2}g^{\mu\nu}\partial_\mu a \partial_\nu a - V(h, a, T)\right]\sqrt{-g}\mathrm{d}^4x. \tag{A.15}$$

The equations of motion now follow from the two Euler-Lagrange equations

$$\frac{\partial \mathcal{L}}{\partial h} - \partial_\mu\left(\frac{\partial \mathcal{L}}{\partial(\partial_\mu h)}\right) = 0, \quad \frac{\partial \mathcal{L}}{\partial a} - \partial_\mu\left(\frac{\partial \mathcal{L}}{\partial(\partial_\mu a)}\right) = 0, \tag{A.16}$$

where each is solved analogously to the method in A.1 to arrive at the two independent equations of motion for the two glueball fields

$$\ddot{h} + 3H\dot{h} + \frac{\partial V_{\text{eff}}(h, a, T)}{\partial h} = 0, \tag{A.17}$$

and

$$\ddot{a} + 3H\dot{a} + \frac{\partial V(h,a,T)}{\partial a} = 0. \tag{A.18}$$

Again, the method to derive the equation for energy density and pressure for two scalar fields are fully analogous to the method in A.1 and we arrive at the equations energy density

$$\rho = \frac{1}{2}(\dot{h}^2 + \dot{a}^2) + V(h,a,T), \tag{A.19}$$

and pressure

$$p = \frac{1}{2}(\dot{h}^2 + \dot{a}^2) - V(h,a,T) \tag{A.20}$$

B Friedmann equation

In this section we derive the Friedmann equation for a flat FLRW universe. This derivation follows the results found in Ref. [22].

An expanding universe follows the Einstein equation

$$R_{\mu\nu} - \frac{1}{2} g_{\mu\nu} R = 8\pi G T_{\mu\nu}, \tag{B.1}$$

where $R_{\mu\nu}$ is the Ricci tensor, $R \equiv g^{\mu\nu} R_{\mu\nu}$ is the Ricci scalar, $g_{\mu\nu}$ is the metric tensor, $T_{\mu\nu}$ is the energy-momentum tensor and G is the gravitational constant.

The Ricci tensor can be described using the Christoffel symbols

$$R_{\mu\nu} = \Gamma^{\alpha}_{\mu\nu,\alpha} - \Gamma^{\alpha}_{\mu\alpha,\nu} + \Gamma^{\alpha}_{\beta\alpha}\Gamma^{\beta}_{\mu\nu} - \Gamma^{\alpha}_{\beta\nu}\Gamma^{\beta}_{\mu\alpha}, \tag{B.2}$$

where the comma notation symbolizes derivatives with respect to x such that $\Gamma^{\alpha}_{\mu\nu,\alpha} \equiv \partial \Gamma^{\alpha}_{\mu\nu} / \partial x^{\alpha}$

The Christoffel symbols are in turn dependent on the metric as follows

$$\Gamma^{\mu}_{\alpha\beta} = \frac{g^{\mu\nu}}{2} \left(\frac{\partial g_{\alpha\nu}}{\partial x^{\beta}} + \frac{\partial g_{\beta\nu}}{\partial x^{\alpha}} - \frac{\partial g_{\alpha\beta}}{\partial x^{\nu}} \right). \tag{B.3}$$

To calculate the symbols we use that the FLRW metric in a spatially flat FLRW universe is

$$g_{\mu\nu} = \begin{pmatrix} 1 & 0 & 0 & 0 \\ 0 & -a^2(t) & 0 & 0 \\ 0 & 0 & -a^2(t) & 0 \\ 0 & 0 & 0 & -a^2(t) \end{pmatrix}. \tag{B.4}$$

The inverse metric is therefore

$$g^{\mu\nu} = \begin{pmatrix} 1 & 0 & 0 & 0 \\ 0 & -1/a^2(t) & 0 & 0 \\ 0 & 0 & -1/a^2(t) & 0 \\ 0 & 0 & 0 & -1/a^2(t) \end{pmatrix}. \tag{B.5}$$

The non-vanishing Christoffel symbols are

$$\Gamma^{0}_{ij} = a\dot{a}\,\delta_{ij}, \qquad \Gamma^{i}_{0j} = \Gamma^{i}_{j0} = \frac{\dot{a}}{a}\delta^{i}_{j}. \tag{B.6}$$

From that, the non-vanishing components of the Ricci tensor are

$$R_{00} = -3\frac{\ddot{a}}{a}, \tag{B.7}$$

and

$$R_{ij} = (a\ddot{a} + 2\dot{a}^2)\delta_{ij}. \tag{B.8}$$

Therefore we find the Ricci scalar is

$$R = -6\left(\frac{\ddot{a}}{a} + \frac{\dot{a}^2}{a^2}\right) \tag{B.9}$$

The energy-momentum tensor for a perfect fluid is

$$T_{\mu\nu} = (\rho + p)u_\mu u_\nu + p g_{\mu\nu}. \tag{B.10}$$

Here, since the fluid is at rest the four-velocity is $u_\mu = (1, 0, 0, 0)$ and therefore the 00-component of the energy-momentum tensor becomes

$$T_{00} = \rho. \tag{B.11}$$

The 00-component of Einstein's equation (B.1) therefore becomes

$$R_{00} - \frac{1}{2} g_{00} R = 8\pi G \rho, \tag{B.12}$$

so we obtain

$$3\left(\frac{\dot{a}}{a}\right)^2 = 8\pi G \rho. \tag{B.13}$$

Defining the Hubble parameter as

$$H \equiv \frac{\dot{a}}{a}, \tag{B.14}$$

we arrive at the Friedmann equation

$$H^2 = \frac{8\pi G}{3}\rho. \tag{B.15}$$

Furthermore, the energy-momentum tensor satisfies the conservation equation

$$\nabla_\mu T^{\mu\nu} = 0, \tag{B.16}$$

which implies

$$\dot{\rho} + 3H(\rho + p) = 0. \tag{B.17}$$

For a relativistic fluid,

$$p = \frac{\rho}{3}, \tag{B.18}$$

such that

$$\dot{\rho} + 4\frac{\dot{a}}{a}\rho = 0. \tag{B.19}$$

Integrating this equation gives

$$\rho \propto \frac{1}{a^4}, \tag{B.20}$$

and since, by (B.15), $\rho \propto H^2$,

$$a(t) \propto t^{1/2}, \tag{B.21}$$

and therefore

$$H = \frac{1}{2t}. \tag{B.22}$$

We then find the relation between the cosmic time and photon temperature by considering the energy density of relativistic particles in thermal equilibrium [23]

$$\rho = g_{*,\rho}(T_\gamma)\frac{\pi^2}{30}T_\gamma^4. \tag{B.23}$$

In natural units we can write $G = m_P^{-2}$, where m_P is the Planck mass, using this and (B.22), (B.15) is then rewritten to find the relation between the cosmic time and photon temperature

$$t = \frac{1}{2}\frac{m_P}{T_\gamma^2}\sqrt{\frac{45}{4\pi^3 g_{*,\rho}(T_\gamma)}}. \tag{B.24}$$

C Cosmological Evolution

Since the temperature T evolves with the cosmic time t, (2.14) can be expanded using the chain rule

$$\dot{\phi} = \frac{\mathrm{d}\phi}{\mathrm{d}T}\frac{\mathrm{d}T}{\mathrm{d}t}. \tag{C.1}$$

Therefore

$$\ddot{\phi} = \frac{\mathrm{d}}{\mathrm{d}t}\left(\frac{\mathrm{d}\phi}{\mathrm{d}T}\frac{\mathrm{d}T}{\mathrm{d}t}\right) = \frac{\mathrm{d}^2\phi}{\mathrm{d}T^2}\left(\frac{\mathrm{d}T}{\mathrm{d}t}\right)^2 + \frac{\mathrm{d}\phi}{\mathrm{d}T}\frac{\mathrm{d}^2T}{\mathrm{d}t^2}. \tag{C.2}$$

To find $\mathrm{d}T/\mathrm{d}t$ we take the derivative of (2.16) with respect to t

$$\begin{aligned}
\frac{\mathrm{d}t}{\mathrm{d}t} = 1 &= \frac{\mathrm{d}}{\mathrm{d}t}\left(\frac{1}{2}\sqrt{\frac{45}{4\pi^3 g_{*,\rho}(T)}}\frac{m_P}{\zeta_T^2 T^2}\right) \\
&= \frac{1}{2}\sqrt{\frac{45}{4\pi^3 g_{*,\rho}(T)}}\frac{m_P}{\zeta_T^2}\frac{\mathrm{d}}{\mathrm{d}t}T^{-2} + \frac{m_P}{\zeta_T^2 T^2}\frac{1}{2}\sqrt{\frac{45}{4\pi^3}}\frac{\mathrm{d}}{\mathrm{d}t}\frac{1}{\sqrt{g_{*,\rho}(T)}} \\
&= \frac{1}{2}\sqrt{\frac{45}{4\pi^3 g_{*,\rho}(T)}}\frac{m_P}{\zeta_T^2}(-2T^{-3})\frac{\mathrm{d}T}{\mathrm{d}t} + \frac{m_P}{\zeta_T^2 T^2}\frac{1}{2}\sqrt{\frac{45}{4\pi^3}}\left(-\frac{1}{2}g_{*,\rho}^{-3/2}(T)\frac{\mathrm{d}T}{\mathrm{d}t}\frac{\mathrm{d}g_{*,\rho}}{\mathrm{d}T}\right) \\
&= -\frac{m_P}{2\zeta_T^2}\sqrt{\frac{45}{4\pi^3}}\left(\frac{1}{\sqrt{g_{*,\rho}(T)}}\frac{2}{T^3}\frac{\mathrm{d}T}{\mathrm{d}t} + \frac{1}{T^2 2 g_{*,\rho}^{3/2}(T)}\frac{\mathrm{d}g_{*,\rho}}{\mathrm{d}T}\frac{\mathrm{d}T}{\mathrm{d}t}\right) \\
&= -\frac{m_P}{2\zeta_T^2}\sqrt{\frac{45}{4\pi^3}}\left(\frac{1}{2g_{*,\rho}^{3/2}(T)T^2}\frac{\mathrm{d}g_{*,\rho}(T)}{\mathrm{d}T}\frac{\mathrm{d}T}{\mathrm{d}t} + \frac{2}{\sqrt{g_{*,\rho}(T)}T^3}\frac{\mathrm{d}T}{\mathrm{d}t}\right) \\
&= -\frac{m_P}{2\zeta_T^2}\sqrt{\frac{45}{4\pi^3}}\frac{\mathrm{d}T}{\mathrm{d}t}\frac{T\frac{\mathrm{d}g_{*,\rho}(T)}{\mathrm{d}T} + 4g_{*,\rho}(T)}{2g_{*,\rho}^{3/2}(T)T^3}
\end{aligned} \tag{C.3}$$

Here we have used the relation $T_\gamma = \zeta_T T$ where T_γ is the photon temperature and T the dark sector temperature. We then assume that $T\frac{\mathrm{d}g_{*,\rho}(T)}{\mathrm{d}T}$ is negligible in comparison to $4g_{*,\rho}(T)$ and therefore we find the derivative of T with respect to t to be

$$\frac{\mathrm{d}T}{\mathrm{d}t} = -\frac{1}{m_P}\sqrt{\frac{4\pi^3 g_{*,\rho}(T)}{45}}\zeta_T^2 T^3. \tag{C.4}$$

The second derivative is therefore

$$
\begin{aligned}
\frac{\mathrm{d}^2T}{\mathrm{d}t^2} &= \frac{\mathrm{d}}{\mathrm{d}t}\left(-\frac{1}{m_P}\sqrt{\frac{4\pi^3 g_{*,\rho}(T)}{45}}\zeta_T^2T^3\right) \\
&= -\frac{1}{m_P}\sqrt{\frac{4\pi^3}{45}}\zeta_T^2\left(\sqrt{g_{*,\rho}(T)}3T^2\frac{\mathrm{d}T}{\mathrm{d}t} + T^3\frac{1}{2}\frac{1}{\sqrt{g_{*,\rho}(T)}}\frac{\mathrm{d}g_{*,\rho}(T)}{\mathrm{d}T}\frac{\mathrm{d}T}{\mathrm{d}t}\right) \\
&= -\frac{-\zeta_T^2}{m_P}\sqrt{\frac{4\pi^3}{45}}\left(\frac{T^3}{2\sqrt{g_{*,\rho}(T)}}\frac{\mathrm{d}g_{*,\rho}(T)}{\mathrm{d}T}\frac{\mathrm{d}T}{\mathrm{d}t} + 3T^2\sqrt{g_{*,\rho}(T)}\frac{\mathrm{d}T}{\mathrm{d}t}\right) \\
&= -\frac{-\zeta_T^2}{m_P}\sqrt{\frac{4\pi^3}{45}}\left(\frac{T^3}{2\sqrt{g_{*,\rho}(T)}}\frac{\mathrm{d}g_{*,\rho}(T)}{\mathrm{d}T} + 3T^2\sqrt{g_{*,\rho}(T)}\right)\left(-\frac{1}{m_P}\sqrt{\frac{4\pi^3 g_{*,\rho}(T)}{45}}\zeta_T^2T^3\right) \\
&= \frac{-\zeta_T^4}{m_P^2}\frac{4\pi^3}{45}T^2\left(\frac{T^3}{2\sqrt{g_{*,\rho}(T)}}\frac{\mathrm{d}g_{*,\rho}(T)}{\mathrm{d}T} + 3T^2\sqrt{g_{*,\rho}(T)}\right) \\
&= \frac{4\pi^3}{45m_P^2}\left(\frac{1}{2}\frac{\mathrm{d}g_{*,\rho}(T)}{\mathrm{d}T}T^6\zeta_T^4 + 3g_{*,\rho}(T)\zeta_T^4T^5\right).
\end{aligned} \tag{C.5}
$$

We then use the expressions (C.4) and (C.5) to rewrite all terms in the equation of motion (2.14) as a function of temperature T in the following way

$$
\ddot{\phi} = \frac{4\pi^3 g_{*,\rho}(T)}{45m_P^2}\zeta_T^4T^6\frac{\mathrm{d}^2\phi}{\mathrm{d}T^2} + \frac{4\pi^3}{45m_P^2}\left(\frac{1}{2}\frac{\mathrm{d}g_{*,\rho}(T)}{\mathrm{d}T}T^6\zeta_T^4 + 3g_{*,\rho}(T)\zeta_T^4T^5\right)\frac{\mathrm{d}\phi}{\mathrm{d}T}. \tag{C.6}
$$

Since the Hubble parameter H can be written

$$
H = \frac{1}{2t} = \sqrt{\frac{4\pi^3 g_{*,\rho}(T)}{45}}\frac{\zeta_T^2T^2}{m_P}, \tag{C.7}
$$

we have

$$
3H\dot{\phi} = -3\zeta_T^4T^5\frac{4\pi^3 g_{*,\rho}(T)}{45m_P^2}\frac{\mathrm{d}\phi}{\mathrm{d}T}. \tag{C.8}
$$

This then gives us the final equation of motion for the glueball field

$$
\frac{4\pi^3 g_{*,\rho}(T)}{45m_P^2}\zeta_T^4T^6\frac{\mathrm{d}^2\phi}{\mathrm{d}T^2} + \frac{2\pi^3}{45m_P^2}\frac{\mathrm{d}g_{*,\rho}(T)}{\mathrm{d}T}\zeta_T^4T^6\frac{\mathrm{d}\phi}{\mathrm{d}T} + \frac{\partial V(\phi,T)}{\partial\phi} = 0 \tag{C.9}
$$

D References

[1] Marco Panero. "Thermodynamics of the QCD plasma and the large-N limit". In: *Phys. Rev. Lett.* 103 (2009), p. 232001. DOI: 10.1103/PhysRevLett.103.232001. arXiv: 0907.3719 [hep-lat].

[2] James Halverson et al. "Gravitational waves from dark Yang-Mills sectors". In: *JHEP* 05 (2021), p. 154. DOI: 10.1007/JHEP05(2021)154. arXiv: 2012.04071 [hep-ph].

[3] Wei-Chih Huang et al. "Testing the dark SU(N) Yang-Mills theory confined landscape: From the lattice to gravitational waves". In: *Phys. Rev. D* 104.3 (2021), p. 035005. DOI: 10.1103/PhysRevD.104.035005. arXiv: 2012.11614 [hep-ph].

[4] Zhaofeng Kang, Jiang Zhu, and Shinya Matsuzaki. "Dark confinement-deconfinement phase transition: a roadmap from Polyakov loop models to gravitational waves". In: *JHEP* 09 (2021), p. 060. DOI: 10.1007/JHEP09(2021)060. arXiv: 2101.03795 [hep-ph].

[5] Pierluca Carenza et al. "Glueball dark matter". In: *Phys. Rev. D* 108.12 (2023), p. 123027. DOI: 10.1103/PhysRevD.108.123027. arXiv: 2306.09510 [hep-ph].

[6] Pierluca Carenza et al. "Glueball Dark Matter Revisited". In: *Phys. Rev. Lett.* 129.26 (2022), p. 261302. DOI: 10.1103/PhysRevLett.129.261302. arXiv: 2207.13716 [hep-ph].

[7] Pierluca Carenza, Roman Pasechnik, and Zhi-Wei Wang. "Composite Heavy Axion-like Dark Matter". In: *Phys. Rev. Lett.* 135.2 (2025), p. 021001. DOI: 10.1103/49pk-z8c8. arXiv: 2408.14245 [hep-ph].

[8] Benjamin Svetitsky and Laurence G. Yaffe. "Critical behavior at finite-temperature confinement transitions". In: *Nuclear Physics B* 210.4 (1982), pp. 423–447. ISSN: 0550-3213. DOI: https://doi.org/10.1016/0550-3213(82)90172-9. URL: https://www.sciencedirect.com/science/article/pii/0550321382901729.

[9] Francesco Sannino. "Polyakov loops versus hadronic states". In: *Phys. Rev. D* 66 (2002), p. 034013. DOI: 10.1103/PhysRevD.66.034013. arXiv: hep-ph/0204174.

[10] Robert D. Pisarski. "Tests of the Polyakov loops model". In: *Nucl. Phys. A* 702 (2002). Ed. by F. Karsch and H. Satz, pp. 151–158. DOI: 10.1016/S0375-9474(02)00699-1. arXiv: hep-ph/0112037.

[11] J. Schechter. "Effective Lagrangian with Two Color Singlet Gluon Fields". In: *Phys. Rev. D* 21 (1980), pp. 3393–3400. DOI: 10.1103/PhysRevD.21.3393.

[12] Joseph Schechter. "Introduction to effective Lagrangians for QCD". In: *eConf* C010815 (2002). Ed. by R. Ouyed and F. Sannino, pp. 76–87. arXiv: hep-ph/0112205.

[13] Lindsay Forestell, David E. Morrissey, and Kris Sigurdson. "Non-Abelian Dark Forces and the Relic Densities of Dark Glueballs". In: *Phys. Rev. D* 95.1 (2017), p. 015032. DOI: 10.1103/PhysRevD.95.015032. arXiv: 1605.08048 [hep-ph].

[14] Biagio Lucini, Antonio Rago, and Enrico Rinaldi. "SU(N_c) gauge theories at deconfinement". In: *Phys. Lett. B* 712 (2012), pp. 279–283. DOI: 10.1016/j.physletb.2012.04.070. arXiv: 1202.6684 [hep-lat].

[15] R. Gomm et al. "Scale Anomaly and the Scalars". In: *Phys. Rev. D* 33 (1986), p. 801. DOI: 10.1103/PhysRevD.33.801.

[16] Rachid Ouyed and Francesco Sannino. "The Glueball sector of two flavor color superconductivity". In: *Phys. Lett. B* 511 (2001), pp. 66–73. DOI: 10.1016/S0370-2693(01)00444-0. arXiv: hep-ph/0103168.

[17] David Curtin, Caleb Gemmell, and Christopher B. Verhaaren. "Simulating glueball production in Nf=0 QCD". In: *Phys. Rev. D* 106.7 (2022), p. 075015. DOI: 10.1103/PhysRevD.106.075015. arXiv: 2202.12899 [hep-ph].

[18] R. L. Workman et al. "Review of Particle Physics". In: *PTEP* 2022 (2022), p. 083C01. DOI: 10.1093/ptep/ptac097.

[19] C. Rosenzweig, J. Schechter, and C. G. Trahern. "Is the Effective Lagrangian for QCD a Sigma Model?" In: *Phys. Rev. D* 21 (1980). Ed. by E. Brezin and S. R. Wadia, p. 3388. DOI: 10.1103/PhysRevD.21.3388.

[20] Eric D. Carlson, Marie E. Machacek, and Lawrence J. Hall. "Self-interacting dark matter". In: *Astrophys. J.* 398 (1992), pp. 43–52. DOI: 10.1086/171833.

[21] James Halverson, Brent D. Nelson, and Fabian Ruehle. "String Theory and the Dark Glueball Problem". In: *Phys. Rev. D* 95.4 (2017), p. 043527. DOI: 10.1103/PhysRevD.95.043527. arXiv: 1609.02151 [hep-ph].

[22] Scott Dodelson. *Modern Cosmology.* Amsterdam: Academic Press, 2003, pp. 57–61. ISBN: 978-0-12-219141-1.

[23] Edward W. Kolb and Michael S. Turner. *The Early Universe.* Addison-Wesley, 1990, pp. 60–65.